On a new two-dimensional Compton camera modality: image reconstruction by back-projection and TSVD

Javier CEBEIRO[1,2], Quentin LEBAILLY[2], Marcela A. MORVIDONE[1], Mai K. NGUYEN[2]

[1]Centro de Matemática Aplicada, Universidad Nacional de San Martín,
Av. 25 de Mayo y Francia, B1650HMP, Gral. San Martín, Buenos Aires, Argentina

[2]Equipes de Traitement de l'Information et Systèmes (ETIS), ENSEA/ Université de Cergy-Pontoise
/UMR CNRS 8051, F-95014 Cergy-Pontoise Cedex, France

jcebeiro@unsam.edu.ar, quentin.lebailly@hotmail.com, mmorvidone@unsam.edu.ar,
mai.nguyen-verger@u-cergy.fr

Résumé – Le concept de caméra Compton a été introduit dans le but d'améliorer notablement la sensibilité des systèmes d'imagerie par rayonnement ionisant conventionnels équipés des collimateurs mécaniques. Dans ce cas, la formation d'images est modélisée par la transformation de Radon sur des cônes dont l'axe pivote autour d'un point (TRCAP). Les données sont des projections coniques tridimensionnelles. Comme l'inversion analytique de cette TRCAP n'est pas connue à l'heure actuelle, nous considérons, dans ce travail, une modalité particulière de caméra Compton en deux dimensions dans laquelle les données enregistrées sont exprimées comme intégrales de la densité de radio-traceur sur des lignes brisées en forme de lettre V ayant un axe pivotant autour d'un point fixe. La reconstruction d'images est réalisée par la méthode de rétroprojection et par la décomposition en valeurs singulières tronquées. Les résultats de simulations sont présentés illustrant la viabilité de cette nouvelle imagerie.

Abstract – Compton cameras have been proposed in order to increase sensitivity in conventional radiation imaging equipped with hole collimators. However, one must deal directly with three dimensional conical projections, which poses the inversion problem for integral data on cone surfaces which does not have so far an analytic solution. In an attempt to clarify this situation, we consider a new two-dimensional Compton camera in which the data are collected as integrals of the radio-tracer on broken lines, actually rotating V-lines, whose vertex is on a circular arch. In the absence of an inversion formula, we present simulation results obtained from a back-projection technique and truncated singular value decomposition.

1 Introduction

Electronic collimation has been proposed in [1] with the objective of improving the efficiency of conventional tomographic emission systems equipped with hole collimators. In this modalities, photons undergoing scattering are considered as noise and rejected with the consequent inefficient usage of radiation. In this configuration, high sensitivity detectors must be used in order to get images based on the energy of scattered photons [2, 3]. Nevertheless, these detectors may be expensive and it would be difficult to integrate them as needed. New modalities should be explored in order to enable different configurations of detectors. In this paper we present a new version of Compton camera with two types of detectors : a single, central, absorption detector and a circular array of scattering detectors. Succinctly, the system operates as follows : a photon scattered at the circular array is detected in coincidence with the central, absorption detector. The measured energy gives information of the angle of the incoming photon. A full set of measures may enable an exact reconstruction of the object under study.

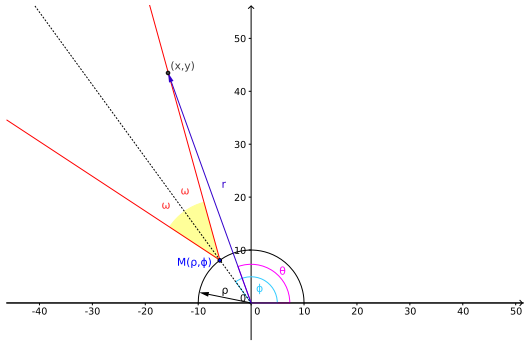

FIGURE 1 – Scheme and coordinates system used in the $R\mathbb{V}T$.

2 A novel approach to a two-dimensional Compton Camera

Consider a bounded-supported function $f(r, \theta)$ in polar coordinates defined in the upper half-plane and representing an object containing a non-uniform radioactivity source distribution. We study a new two-dimensional Compton camera with a

scattering detector in the form of half a circle of radius ρ and a point-like absorption detector. Both detectors are centred at the origin of coordinates O (see Fig. 1). The coincidence detection of a scattering event on the semi-circle detector and of an absorption at O, allows not only to know the angular coordinate ϕ of the scattering site M, but also to register the number of single scattered radiation at an energy E (i.e. the scattering angle ω).

2.1 The Radon transform on Rotating $\mathbb{V}$-lines ($R\mathbb{V}T$)

According to the process of generation of data described in Sec. 2, the amount of radiation at O can be expressed as the integral of the activity distribution on two half lines meeting at M and making an angle ω with the line OM. The result is a broken line with opening angle ω. The angle ω is measured between each branch of the V-line and the symmetry axis as it is shown in Fig. 1. Because of the fact that this symmetry axis rotates around O, the transform is a Radon Transform on Rotating $\mathbb{V}$-lines ($R\mathbb{V}T$) and its expression is given by :

$$g(\phi,\omega) = \int_{\rho}^{\infty} \frac{dr}{\sqrt{1-(\frac{\rho\sin\omega}{r})^2}} \left[f(r, \cos^{-1}\frac{\rho\sin\omega}{r} + \phi - \frac{\pi}{2} + \omega) + f(r, -\cos^{-1}\frac{\rho\sin\omega}{r} + \phi + \frac{\pi}{2} - \omega) \right], \quad (1)$$

where $\phi \in (0,\pi)$, $\omega \in (-\frac{\pi}{2}, \frac{\pi}{2})$ and $g(\phi,\omega)$ are the data measured at site ϕ corresponding to a scattering angle ω.

2.2 The Point Spread Function

The idea described above can be alternatively written as a double integral by means of the Point Spread Function ($\text{PSF}_{R\mathbb{V}T}$) :

$$g(\phi,\omega) = \int\int dr\, d\theta\ \text{PSF}_{R\mathbb{V}T}(\phi,\omega|r,\theta) f(r,\theta). \quad (2)$$

The $\text{PSF}_{R\mathbb{V}T}$ is the impulse response of the operator $R\mathbb{V}T$, the substitution $f(r,\theta) = \frac{1}{r}\delta(r-r_0)\delta(\theta-\theta_0)$ in (1) leads to :

$$\text{PSF}_{R\mathbb{V}T}(\phi,\omega|r_0,\theta_0) = \frac{1}{\sqrt{r_0^2-(\rho\sin\omega)^2}} \left[\delta(\cos^{-1}\frac{\rho\sin\omega}{r_0} + \phi - \frac{\pi}{2} + \omega - \theta_0) + \delta(-\cos^{-1}\frac{\rho\sin\omega}{r_0} + \phi + \frac{\pi}{2} - \omega - \theta_0) \right]. \quad (3)$$

Clearly, because of the Delta functions in (3), the $\text{PSF}_{R\mathbb{V}T}$ is supported by a curve of equation :

$$\omega = \tan^{-1}\left(\pm \frac{r_0\sin(\theta_0-\phi)}{\rho - r_0\cos(\theta_0-\phi)} \right), \quad (4)$$

in the plane (ϕ,ω). Singularities in (4) indicate the scanning limits, i.e. an angular interval (ϕ_{min},ϕ_{max}) where a given point (r_0,θ_0) can project to. For additional discussion and examples on support and scanning limits refer to [4].

3 Reconstruction Techniques

3.1 Back-projection

It is broadly known that in some line integral transforms, inverse formulas can be written in the form of filtered back-projection of the measurement data [2]. In this section we shall apply a single (i.e. not filtered) back-projection algorithm in order to obtain an approximate image reconstruction. First of all, we describe the underlying idea of back-projection in the simplest case (CRT). For a given angle ω, the back-projected image $R_w(x_0,y_0)$ is generated by assigning to the point (x_0,y_0) the value that the projection takes at the position in the array detector to which this point projects [5]. Afterwards all back-projected images $R_w(x_0,y_0)$ are integrated in order to obtain the summation image yielding an approximate image of the original object. This integration procedure is often called summation of back-projections. Back-projection is an important intermediate step in many reconstruction algorithms [6], even some older experimental computed tomography systems used it as reconstruction technique [7]. Of course, it is necessary to do this for every (x,y) in order to obtain the approximation $\tilde{f}(x,y)$ of the image. Nevertheless, extra filtering may be needed because $\tilde{f}(x,y)$ is not the original image since the process is not an exact inversion. Fig. 2 shows the extension of the geometric idea for the case of the $R\mathbb{V}T$. According to equation (1), for a given scattering angle ω, point (x_0,y_0) in the figure projects to the detector at two angles : ϕ_1 and ϕ_2. It is intuitive and straightforward to assign to the point (x_0,y_0) the sum of those values corresponding to the projections at angles ϕ_1 and ϕ_2 as in equation (5). The idea is the same as the one explained above but, as the transform changes, the back-projection is the addition of projections at two points on the semi-circular scattering detector :

$$R_w(x_0,y_0) = g(\phi_1,\omega) + g(\phi_2,\omega). \quad (5)$$

These angles correspond to the point at which the straight lines meeting at point (x_0,y_0) cross the circular detector of radius ρ. Let's consider the central branches in Fig. 2, the right branch of the green "V" and the left branch of the red "V". They intersect at (x_0,y_0) and its equations are : $y = y_0 + (x - x_0)\tan(\phi_1+\omega)$ and $y = y_0 + (x-x_0)\tan(\phi_2-\omega)$. Taking into account that both lines pass through the points (x_0,y_0) and $(\rho\cos\phi, \rho\sin\phi)$, where ϕ is ϕ_1 and ϕ_2 respectively, we arrive to the following equation for ϕ_1 :

$$\begin{pmatrix} x_0 - y_0\cot\omega \\ y_0 + x_0\cot\omega \end{pmatrix} \begin{pmatrix} \cos\phi_1 \\ \sin\phi_1 \end{pmatrix} = \rho. \quad (6)$$

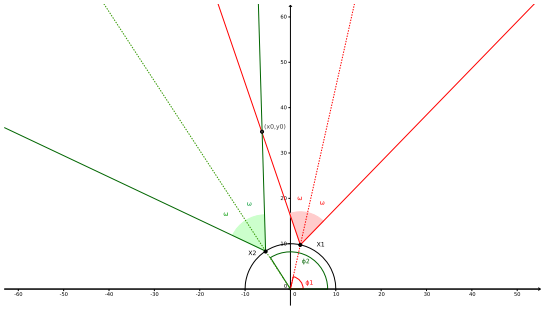

FIGURE 2 – Geometrical interpretation of back-projection

We obtained an equivalent expression for ϕ_2, each of them having two solutions. Using geometrical criteria, we obtain the values for angles ϕ_1 and ϕ_2 :

$$\phi_{1,2} = \arctan \frac{y_0 \pm x_0 \cot\omega}{x_0 \mp y_0 \cot\omega} \mp \arccos\left(\frac{\rho}{\sqrt{(x_0 \mp y_0\cot\omega)^2 + (y_0 \pm x_0\cot\omega)^2}}\right). \quad (7)$$

Then, having the angles ϕ_1 and ϕ_2, we are able to calculate the back-projection (5). Finally, the approximate image is obtained by integration of all back-projections labelled by ω :

$$\tilde{f}(x_0, y_0) = \int_{-\frac{\pi}{2}}^{\frac{\pi}{2}} d\omega \;\; R_\omega(x_0, y_0). \quad (8)$$

3.2 Matrix Inversion

The $R\mathbb{V}T$ as a Linear System The matrix formulation of the direct problem described above reads :

$$\mathbf{g} = A\mathbf{f}. \quad (9)$$

Here $\mathbf{g}$ is the projection vector, each of its components is a projection value, and its size is $N_\phi N_\omega \times 1$. Vector $\mathbf{f}$ represents the object of interest, its size is equal to the number of pixels $N^2 \times 1$, and finally A is the projection matrix of size $N_\phi N_\omega \times N^2$. There is a strong link between (1) and (9) since : columns in matrix A are generated with formula (3), $\mathbf{g} = g(\phi, \omega)$, $\mathbf{f} = f(x, y)$ and the product $A\mathbf{f}$ represents the $R\mathbb{V}T$ itself. The algebraic formulation can be understood as a discrete version of equation (2).

Inversion Using Truncated Singular Value Decomposition In the problem presented in the form (9), inversion consists in finding the original function $\mathbf{f}$ from projection data $\mathbf{g}$. The Singular Value Decomposition (SVD) is a non-iterative method which enables algebraic inversion of $A_{m\times n}$ ($m \geq n$) through factorization in the form $A = U_{m\times m} \times S_{m\times n} \times V^t_{n\times n}$, where U and V are orthogonal matrices whose columns are eigenvectors of AA^t and A^tA respectively and S is a diagonal matrix

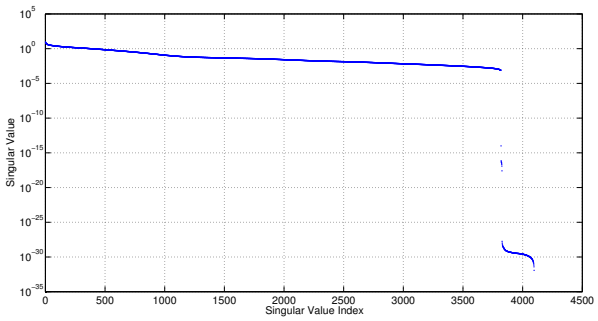

FIGURE 3 – SVD spectrum of matrix A generated with the $\text{PSF}_{R\mathbb{V}T}$ formula.

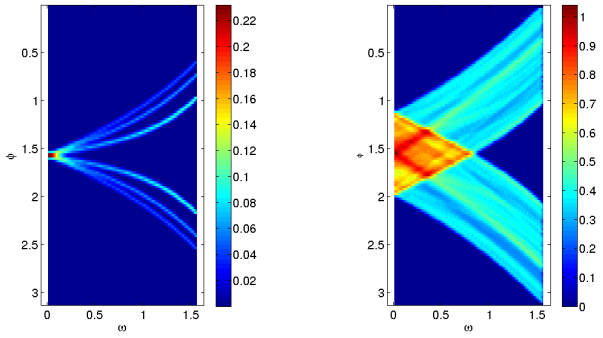

FIGURE 4 – Projections : punctual sources (left) and Shepp-Logan-like image (right).

containing the singular values of A. This factorization allows us to write the pseudo inverse $A^\dagger = V \times S^{-1} \times U^t$ and thus the inversion problem is solved. Sometimes, when matrix A is ill-conditioned, it is possible to overcome the ill-posedness of the problem through an appropriate truncation of the smallest singular values. This technique is called Truncated Singular Value Decomposition (TSVD). For a detailed description of this method as well as its imaging applications see [8–10].

4 Numerical Simulations

In order to test the imaging capabilities of the new modality, we performed numerical simulations. In this first stage, only noiseless conditions were considered. A Compton camera with $N_\phi = 128$ elements in a semicircular detector of radius $\rho = 13$ was considered. The number of measured angles (energies) was set to $N_\omega = 128$. Matrix $A_{16384\times4096}$ was generated using the $\text{PSF}_{R\mathbb{V}T}$ formula (3) where Dirac functions were approximated using a symmetric-triangular function with unit area and supported in the interval $(-0.05, 0.05)$. The nature of the inversion problem was ill-posed. Although A was ill-conditioned ($k = 1.5\ 10^{20}$), its numerical rank was well-determined, see classification in [8]. The gap in the SVD spectrum in Fig. 3

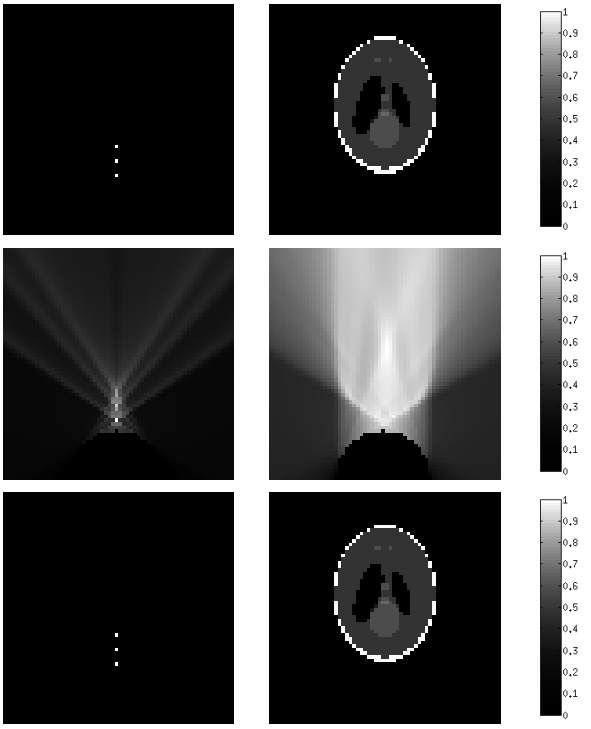

FIGURE 5 – Upper : original testing images, three points and Shepp Logan. Middle : back-projections. Down : reconstructions using TSVD.

suggests that T=3818 is the best truncation index for pseudo-inversion in TSVD, [10]. Projections were calculated using (9) and are shown in Fig. 4. Two square images ($N \times N = 64 \times 64$) were considered : an image inspired in the Shepp-Logan phantom and a simpler image consisting of three-points (Fig. 5). Reconstructions were performed using the two methods explained above. Numerical integration in the back-projection algorithm was carried out with a step $\Delta\omega = 0.024$. Matrix inversion was performed using TSVD, with $T = 3818$. Figure 5 shows the results of reconstruction for both cases.

5 Conclusions

According to the results obtained in numerical simulations, this new two-dimensional Compton camera modality offers interesting possibilities. There is still significant progress to be done before it turns into a real exploitable imaging device. Although images reconstructed using back-projection exhibit significant blurring, results suggest that further work should be done in order to find appropriate filters for a filtered back-projection algorithm. Work in this direction is in progress. A further study under more realistic conditions should be performed in order to determine the proper treatment to this problem (dominant type of noise as well as denoising strategies). In addition, further studies in order to determinate the influence of the physical features of the detection system should be done : the radius ρ of the arch detector, the best number of energies (N_ω) and detectors (N_ϕ), etc. For comparison purposes, results obtained with iterative algebraic methods can be found elsewhere [4].

Acknowledgements

Javier Cebeiro research work is supported by a CONICET grant, he also acknowledges support from Programa BEC.AR for financial funding of a visit in 2015 to laboratory Equipes de Traitement de l'Information et Sysèms (ETIS)-ENSEA / Université de Cergy-Pontoise/ CNRS UMR 8051, France. Marcela Morvidone was supported in part by SOARD-AFOSR Grant FA9550-14-1-0276. The authors also thank Diana Rubio and Tuong Truong for stimulating discussions.

Références

[1] M. Singh. *An electronically collimated gamma camera for single photon emission computed tomography. Part 1 : Theoretical considerations and design criteria* Med. Phys., vol. 10, pp. 421-427, 1983.

[2] M. Morvidone, M. Nguyen, T. Truong, and H. Zaidi. *Scattered Radiation , Emission Imaging : Principles and Applications.*, International Journal of Biomedical Imaging. Vol. 2011.

[3] M. Nguyen and T. Truong. *Imagerie par rayonnement gamma diffusé.*, Hermes, 2005.

[4] J. Cebeiro Q. Lebailly M. Morvidone and M. Nguyen. *A new modality of bidimensional Compton camera.* 37th Conference EMBS IEEE, Milano, Italy, August, 2015.

[5] H. Barrett. *The Radon Transform and its Applications.* Progress in Optics, 21, North Holland, 1984.

[6] S. Deans. *The Radon Transform and Some of Its Applications.* Mineola, New York : Dover Publications, 2007.

[7] R. Gonzalez and R. Woods. *Digital Image Processing 3rd. Edition.* Addison Wesley, 2009.

[8] C. Hansen. *The truncated SVD as a method for regularization.* BIT Num. Mathematics, Vol. 27, Springer, 1987.

[9] V. Selivanov and R. Lecomte. *Fast PET image reconstruction based on SVD decomposition of the system matrix.* IEEE, Trans. Nucl. Sci., vol 48, 2001.

[10] J. Cebeiro and M. Morvidone. *SVD inversion for the bidimensional Conical Radon Transform.* Journal of Physics : Conference Series, Volume 477, 2013.